ISSN 1063-7745, Crystallography Reports, 2008, Vol. 53, No. 7, pp. 1124–1132. © Pleiades Publishing, Inc., 2008.

REAL STRUCTURE OF CRYSTALS

Modeling of the Defect Structure in Dislocation-Free Silicon Single Crystals

V. I. Talanin, I. E. Talanin, and A. A. Voronin

University of State and Municipal Government, Zaporozhye, 69002 Ukraine

e-mail: v.i.talanin@mail.ru

Received November 3, 2006

Abstract—A mathematical model of the formation of primary grown-in microdefects on the basis of dissociation diffusion is presented. Cases of "vacancy–oxygen" (V + O) and "carbon–interstitial" (C + I) interaction near the crystallization front are considered for dislocation-free Si single crystals grown by the floating-zone and Czochralski methods. The approximate analytical expressions obtained by setting 1D and 2D temperature fields in a crystal are in good agreement with the heterogeneous mechanism of formation of grown-in microdefects.

PACS numbers: 61.72.Bb; 61.72.Ji; 61.72.Yx.

DOI: 10.1134/S1063774508070055

INTRODUCTION

Grown-in microdefects determine not only the initial defect structure of dislocation-free Si single crystals but also the subsequent processes of its transformation as a result of technological processes. Therefore, investigation of the mechanism of formation of grown-in microdefects is a key both to controlling the defect structure of crystals and to understanding the problem of fundamental interactions of point defects.

Currently, there are two approaches to solution of the problem of grown-in microdefect formation. The first approach has been developed within the model of dynamics of point defects, in which a crystal is considered as a dynamic system or a solid-state chemical reactor, in which point defects move and interact. It is assumed that modeling of the dynamics of point defects makes it possible to understand quantitatively the processes of formation of grown-in microdefects and their spatial distribution [1]. The model of point-defect dynamics involves convection, diffusion, and recombination of intrinsic point defects. In this model, the process of fast recombination of intrinsic point defects near the melting temperature plays a crucial role. The reason is that the modifications of the model of point-defect dynamics [2, 3] are based on Voronkov's theoretical model of grown-in microdefect formation [4]. Voronkov assumed that (i) the recombination rate of intrinsic point defects near the melting point is very high, (ii) the diffusion coefficient of Si interstitials near the melting point exceeds the vacancy diffusion coefficient, and (iii) the equilibrium vacancy concentration near the melting point exceeds the equilibrium interstitial concentration. He showed that grown-in microdefect formation is controlled by the growth parameter $C_{crit} = V/G$ (where V is the crystal growth rate and G is the axial temperature gradient). This theoretical model describes the formation of vacancy micropores (vacancy clusters) at $V/G > C_{crit}$ and interstitial dislocation loops at $V/G < C_{crit}$ in different regions of a crystal. In view of this finding, all modifications of the model of point-defect dynamics a priori assume that all types of grown-in microdefects (A, B, D(C) microdefects and vacancy micropores) are manifestations of different stages of formation of only two types of grown-in microdefects: vacancy micropores and interstitial dislocation loops. Therefore, it was concluded that grown-in microdefect formation is based on the decomposition of a supersaturated solid solution of intrinsic point defects (vacancies and Si interstitials), which occurs upon crystal cooling from the crystallization temperature. One should take into account that, despite the subsequent modification [5], a significant drawback of the Voronkov model and, respectively, the model of point-defect dynamics is that it disregards the interaction between impurities and intrinsic point defects.

The second approach is related to the results of experimental investigations of the physical nature and characteristics of grown-in microdefects [6]. On the basis of these experimental data, we constructed a qualitative heterogeneous mechanism of formation and transformation of grown-in microdefects, which is based on the following statements [7]:

(i) Recombination of intrinsic point defects near the melting point is negligible owing to the presence of a recombination barrier.

(ii) Background oxygen and carbon impurities are directly involved in the formation and transformation of grown-in microdefects.

(iii) Decomposition of a supersaturated solid solution of point defects upon cooling a crystal occurs via two mechanisms: vacancy and interstitial.

The basic concepts of the heterogeneous mechanism contradict the theoretical statements of the Voronkov model. There is a large amount of experimental data confirming the adequacy of this mechanism to the real processes of defect formation in dislocation-free Si single crystals. At the same time, the heterogeneous mechanism also has a significant drawback: the absence of a corresponding mathematical model. In this context, the purpose of this study was to justify the theoretical model of the heterogeneous mechanism of grown-in microdefect formation as a result of the "impurity–intrinsic point defect" interaction.

1. PHYSICAL MODEL

It was shown that the driving force of defect formation is oxygen–vacancy and carbon–interstitial agglomerates formed on the basis of impurity centers [7]. It was experimentally found that the formation of oxygen–vacancy and carbon–interstitial agglomerates ((I + V) microdefects) begins near the melting point [6]. It is known that secondary grown-in microdefects are formed upon cooling a crystal at temperatures below 1200°C [8]. On the basis of these experimental results, we introduced the concepts of primary grown-in microdefects ((I + V), D(C), B microdefects) and secondary grown-in microdefects (A microdefects, vacancy micropores), involving the following types of interaction: primary (fundamental) "impurity–intrinsic point defect" and secondary ("intrinsic point defect—intrinsic point defect"), respectively.

We propose to consider the defect structure of a crystal as a structure composed of two subsystems: primary and secondary grown-in microdefects. It is assumed that the subsystem of secondary defects (vacancy micropores and interstitial dislocation loops) can be described by the Voronkov model. In this study, we consider the process of formation of primary grown-in microdefects.

As was noted above, in dislocation-free Si single crystals grown by the floating-zone (FZ-Si) and Czochralski (CZ-Si) methods, the recombination of intrinsic point defects near the crystallization front is negligible owing to the presence of an entropy recombination barrier [6, 8]. At temperatures close to the melting point, equilibrium concentrations of vacancies and Si interstitials exist simultaneously. Hence, decomposition of the supersaturated solid solution of point defects occurs simultaneously via two mechanisms. In correspondence with the sign of the elastic strain of the silicon lattice, these mechanisms were referred to as vacancy and interstitial. According to the heterogeneous mechanism of grown-in microdefect formation, vacancies (V) and Si interstitials (I) find sinks in the form of background oxygen (O) and carbon (C) impurities, respectively. In the initial stage of defect formation, these processes lead to the appearance of (V + O) and (C + I) complexes. One can write the following quasichemical equations for the vacancy and interstitial branch of the heterogeneous mechanism: $O_i + V \longrightarrow (O + V)$ and $C_S + I \longrightarrow (C + I)$, respectively ($O_i$ are oxygen interstitials and C_S are carbon substituents).

Such an idealized system is characteristic of undoped FZ-Si single crystals grown in vacuum with an impurity concentration less than 5×10^{15} cm^{-3}. One should take into account that such a system disregards the possibility of joint interaction of O_i and C_S. In addition, considering commercial FZ-Si and CZ-Si crystals, one has to take into account the presence and interaction of other point defects (for example, iron, nitrogen, dopants).

In this study, we consider an idealized system for four variables (vacancies, interstitials, oxygen, and carbon).

2. MATHEMATICAL MODEL

The solution is sought within the model of dissociative diffusion–migration of impurities [9]. In this case, the difference from the decomposition phenomenon is that during diffusion (as a technological process), a diffusant is supplied to the sample from an external source, whereas in the case of decomposition it is produced by an internal source (lattice sites). The theoretical analysis in the same; however, in deformation of dissociative diffusion, one has to take into account the surface concentration, which decreases in the sample volume with time and along the coordinate. The time constant is determined by the migration mechanism in the sample volume, while the coordinate dependence is determined by the sample shape and the boundary conditions of the diffusion problem.

It is difficult to interpret diffusion in multicomponent systems because it is necessary to take into account the interaction of impurity atoms. Generally, one has to use numerical methods to solve the equations; simple analytical expressions, convenient for comparison with the experimental data, can be obtained only in certain approximations. The mechanism of complex formation can be different; however, independent of the nature of the forces leading to the formation of complexes, any model assumes the action radius of these forces to be small. In this case, in analysis of the migration of point defects, a complex can be considered as a point defect.

Let us write the formation of complexes as a quasichemical reaction

$$A + B \longleftrightarrow AB. \quad (1)$$

Then, the thermodynamic equilibrium condition between the free impurities A and B and the impurity bound into AB complexes can be written in the form

$$\mu_A + \mu_B = \mu_{AB}, \tag{2}$$

where μ_A and μ_B are the chemical potentials of free impurities and μ_{AB} is the chemical potential of complexes.

If the total concentration of A and B impurities (N_A, N_B) is low in comparison with the concentration of the main material, $\mu_{AB} \approx \ln N_{AB}$ in this approximation, and the equilibrium condition (2) can be written as

$$\frac{(N_A - Q)(N_B - Q)}{Q} = k(T), \tag{3}$$

where Q is the concentration of complexes and $k(T)$ is the constant of the complex formation reaction, which is temperature-dependent (at constant pressure) [10]. At $k = 0$, the impurity is totally bound into complexes (strong complex formation).

One should take into account that, in the diffusion equations written with allowance for the complex formation, the total impurity flux is the sum of the free impurity flux and the flux of the impurity bound into complexes [10]:

$$\frac{\partial N_A}{\partial t} = D_A\frac{\partial^2(N_A - Q)}{\partial x^2} + D_Q\frac{\partial^2 Q}{\partial x^2}, \tag{4}$$

$$\frac{\partial N_B}{\partial t} = D_B\frac{\partial^2(N_B - Q)}{\partial x^2} + D_Q\frac{\partial^2 Q}{\partial x^2}, \tag{5}$$

where D_A, D_B, and D_Q are the diffusion coefficients of the free components A and B and complexes, respectively; x is the coordinate (crystal length); and t is time.

The diffusion coefficient of complexes depends on the mechanism of complex formation and the type of their components. In particular, if a complex consists of two interacting atoms, the diffusion coefficient D_Q is much smaller than the corresponding diffusion coefficients of these atoms, D_A and D_B. Therefore, assuming the complexes to be low-mobile, one can neglect the last terms in Eqs. (4) and (5):

$$\frac{\partial N_A}{\partial t} = D_A\frac{\partial^2(N_A - Q)}{\partial x^2}, \tag{6}$$

$$\frac{\partial N_B}{\partial t} = D_B\frac{\partial^2(N_B - Q)}{\partial x^2}. \tag{7}$$

Complexes are immobile; hence, the boundary conditions are written for the free impurity. Since the equilibrium settling time for the complexes and free impurity is much shorter than the characteristic diffusion time, the total impurity concentration can be set as the initial condition.

Vas'kin and Uskov [10] considered the problem of successive diffusion of a component A into a sample singly doped with a component B, taking into account the complex formation at the initial and boundary conditions:

$$\begin{aligned} N_A(x, 0) &= 0 \\ N_B(x, 0) &= N_B(\infty) \\ N_A(0, t) - Q(0, t) &= H_A(0) \\ \frac{\partial}{\partial x}[N_B(x, t) - Q(x, t)]_{x=0} &= 0. \end{aligned} \tag{8}$$

In this case, the diffusion equation has the form

$$\left.\begin{aligned} &\frac{1}{2}[N_A - N_B - k \\ &+ \sqrt{k^2 + 2k(N_A + N_B) + (N_A - N_B)^2}]'' \\ &+ 2\lambda N_A' = 0 \\ &\frac{1}{2}[N_B - N_A - k \\ &+ \sqrt{k^2 + 2k(N_A + N_B) + (N_A - N_B)^2}]'' + 2\lambda d^2 N_B' \end{aligned}\right\}, \tag{9}$$

where $\lambda = \dfrac{x}{2\sqrt{D_A t}}$ is the Boltzmann substitution, primes denote differentiation with respect to λ, and $d^2 = \dfrac{D_A}{D_B}$.

The solution to the system of equations (9) with the corresponding boundary conditions (diffusion of the impurity A from a constant source into a semiconductor that is homogeneously doped with the impurity B; the impurity B does not evaporate) in the case of strong complex formation ($k = 0$) is [10]

$$N_A = \begin{cases} N_{B1} + H_A(0)\left[1 - \dfrac{\operatorname{erf}(\lambda/d_A)}{\operatorname{erf}(\lambda_0/d_A)}\right], & \lambda < \lambda_0 \\ 0, \quad \lambda > \lambda_0, \end{cases} \tag{10}$$

$$N_B = \begin{cases} N_{B1}, \quad \lambda < \lambda_0 \\ N_{B0}\left(1 - \dfrac{\operatorname{erfc}(\lambda d)}{\operatorname{erfc}(\lambda_0 d)}\right), & \lambda > \lambda_0, \end{cases} \tag{11}$$

where

$$N_{B1} = \frac{N_{B0}e^{-\lambda_0 d^2}}{\sqrt{\pi}\lambda_0 d \operatorname{erfc}(\lambda_0 d)}; \tag{12}$$

λ_0 is derived from the equation

$$\frac{e^{\lambda_0^2(1-d^2)}\operatorname{erf}(\lambda_0)}{\operatorname{erfc}(\lambda_0 d)} = \frac{N_{A0}}{N_{B0}}. \quad (13)$$

Let us rewrite the system of equations (3)–(5) for the diffusion impurity kinetics of mobile complexes in terms of total components, $N_A = H_A + Q$ and $N_B = H_B + Q$:

$$d_A^2(N_A - Q)'' + d_Q^2 Q'' + 2\lambda N_A' = 0, \quad (14)$$

$$d_B^2(N_B - Q)'' + d_Q^2 Q'' + 2\lambda N_B' = 0, \quad (15)$$

$$(N_A - Q)(N_B - Q) = k(T)Q. \quad (16)$$

In Eqs. (10)–(16) and below, $d_A^2 = D_A$; $d_B^2 = D_B$; $d_Q^2 = D_Q$. In Eqs. (8)–(16) and below, H_A and H_B are the concentrations of the free impurities A and B and N_{A0} and N_{A0} are the impurity concentrations at the interface.

Note that the solution to the system of equations is considered for the three cases that are most often met in practice: successive distribution, simultaneous diffusion, and interdiffusion. Under the conditions of our physical model, we can speak about successive diffusion, at which the condition of zero flux of one of the components (located at the initial instant in the sample bulk) is set at the interface. In this case, the boundary conditions have the form

$$\begin{aligned} &H_A|_{\lambda=0} = H_A(0); \quad H_A|_{\lambda=\infty} = H_A(\infty) \\ &d_B^2 H_B' + d_Q^2 Q'|_{\lambda=0} = 0; \quad H_B|_{\lambda=\infty} = H_B(\infty). \end{aligned} \quad (17)$$

Generally, the system of equations (14)–(16) with the boundary conditions (17) does not have an analytical solution; therefore, to analyze the shape of the impurity profiles, one has to analyze the limiting cases. Let us consider the approximation of strong complex formation ($k = 0$), which physically means that the $A + B \longleftrightarrow Q$ reaction is significantly shifted toward complex formation. In addition, at $k = 0$, it follows formally from the system of equations (14)–(16) that the concentration of at least one of the free components is zero; i.e., $H_A = 0$ or $H_B = 0$ (the impurity is completely bound into complexes).

The solution to the problem of diffusion of a component A in a semi-infinite sample homogeneously doped with a component B, with the absence of evaporation of the component B from the sample and the presence of the free component A at the sample boundary, has the form [9]

$$H_A = N_A - Q$$
$$= \begin{cases} (N_A(0) - N_{B1})\left[1 - \dfrac{\operatorname{erfc}(\lambda/d_A)}{\operatorname{erfc}(\lambda_0/d_A)}\right], & \lambda \le \lambda_0 \\ 0, \quad \lambda > \lambda_0, \end{cases} \quad (18)$$

$$H_B = N_B - Q$$
$$= \begin{cases} 0, \quad \lambda \le \lambda_0 \\ N_B(\infty)\left[1 - \dfrac{\operatorname{erfc}(\lambda/d_B)}{\operatorname{erfc}(\lambda_0/d_B)}\right], & \lambda > \lambda_0, \end{cases} \quad (19)$$

$$Q = \begin{cases} N_{B1}, \quad \lambda \ge \lambda_0 \\ N_{B1}\dfrac{\operatorname{erfc}(\lambda/d_Q)}{\operatorname{erfc}(\lambda_0/d_Q)}, & \lambda < \lambda_0, \end{cases} \quad (20)$$

$$\begin{aligned} N_{B1}S_1(\lambda_0/d_Q) &= N_B(\infty)S_1(\lambda_0/d_B) \\ N_{B1}S_1(\lambda_0/d_Q) &= \{N_A(0) - N_{B1}\}S_2(\lambda_0/d_A), \end{aligned} \quad (21)$$

where $S_1(x) = \dfrac{\exp(-x^2)}{\sqrt{\pi}x\operatorname{erfc}(x)}$, $S_2(x) = \dfrac{\exp(-x^2)}{\sqrt{\pi}x\operatorname{erf}(x)}$, and $N_A(0) - N_{B1} = H_A(0)$. d_A, d_B, and d_Q are found from Eqs. (14)–(16).

3. EXPERIMENTAL

Under physical-model conditions (heterogeneous mechanism of grown-in microdefect formation), we assume that the component A is the background impurity (oxygen O or carbon C) and the component B is intrinsic point defects (vacancies V or interstitials I). For the vacancy and interstitial mechanisms, we consider, respectively, the oxygen + vacancy (O + V) and carbon + interstitial (C + I) interactions. The following values were used in the calculations:

$$H_A(0) = H_o(0) = 4\times10^{15}\ \text{cm}^{-3}\ \text{(FZ-Si)};$$

$$H_A(0) = H_o(0) = 8\times10^{16}\ \text{cm}^{-3}\text{(CZ-Si)};$$

$$C_V = 8.84\times10^{14}\ \text{cm}^{-3}; \quad D_V = 4\times10^{-5}\ \text{cm}^2/\text{s};$$

$$D_o = 0.17\exp(-2.54/kT),$$

$$k = 8.6153\times10^{-5}\ \text{eV/K},$$

$$H_A(0) = H_c(T_m) = 4\times10^{15}\ \text{cm}^{-3}\ \text{(FZ-Si)},$$

$$H_A(0) = H_c(0) = 1\times10^{16}\ \text{cm}^{-3}\ \text{(CZ-Si)},$$

$$C_I(0) = 6.31\times10^{14}\ \text{cm}^{-3},$$

$$D_I = 4.75\times10^{-4}\ \text{cm}^2/\text{s}, \quad D_c = 1.9\exp(-3.1/kT).$$

The solution to Eqs. (12) and (13) has a physical meaning ($N_{B1} \sim 10^{12}$–10^{14} cm^{-3}) only at $\lambda \approx 0.01$. Note that, in the approximation of strong complex formation, λ_0 is interpreted as the front boundary of the complex formation reaction. Since x is the crystal length and x_0 is the position of the crystallization front, we can con-

Temperatures of formation of microdefects of different types

Growth rate, mm/min	Growth conditions	Type of micro-defects	Distance from the crystallization front, mm	Formation temperature, ±20 K
2	Quenching	A	23	$T_A = 1373$
3	Quenching	B		$T_B = 1653$
6	Quenching	D	26	$T_D = 1423$
6; 9	Quenching	I + V		$T_{I+V} = 1653$

clude that complex formation occurs near the crystallization front.

These calculated data are confirmed by the experimental investigation of the initial stages of defect formation. The experiment was performed with quenching of undoped FZ-Si single crystals 30 mm in diameter, which were grown in vacuum at different growth rates (2, 3, 6, 9 mm/min). One of the most effective methods for crystal quenching was used: decantation of the molten region, which implies sharp blowing out of the zone by a directed argon flow at a certain instant. These experiments made it possible to determine the temperatures of grown-in microdefect formation (Table 1) [6].

Quenching of the FZ-Si crystals grown at V = 6 mm/min leads to the formation of a so-called defect-free region between the crystallization front and the region with D microdefects. The electron microscopy analysis shows that the defect-free region contains both interstitial and vacancy defects 2–7 nm in size with a concentration of ~4.5×10^{13} cm^{-3} ((I + V) microdefects). The FZ-Si crystals grown at V = 9 mm/min, being quenched, exhibit interstitial and vacancy microdefects in comparable concentrations.

Analysis of the detachment surface revealed that, owing to the thermal impact, dislocations arise at distances no more than 1–3 mm from the crystallization front. Therefore, it is difficult to determine exactly the onset of the formation of primary grown-in microdefects. Taking into account this circumstance and proceeding from the data of Table 1, we can state that primary grown-in microdefects are formed near the crystallization front.

Figure 1 shows the dependences of the temperature distribution on the crystal length $T(x)$ for FZ-Si (30 mm in diameter) and CZ-Si (50 mm in diameter) crystals.

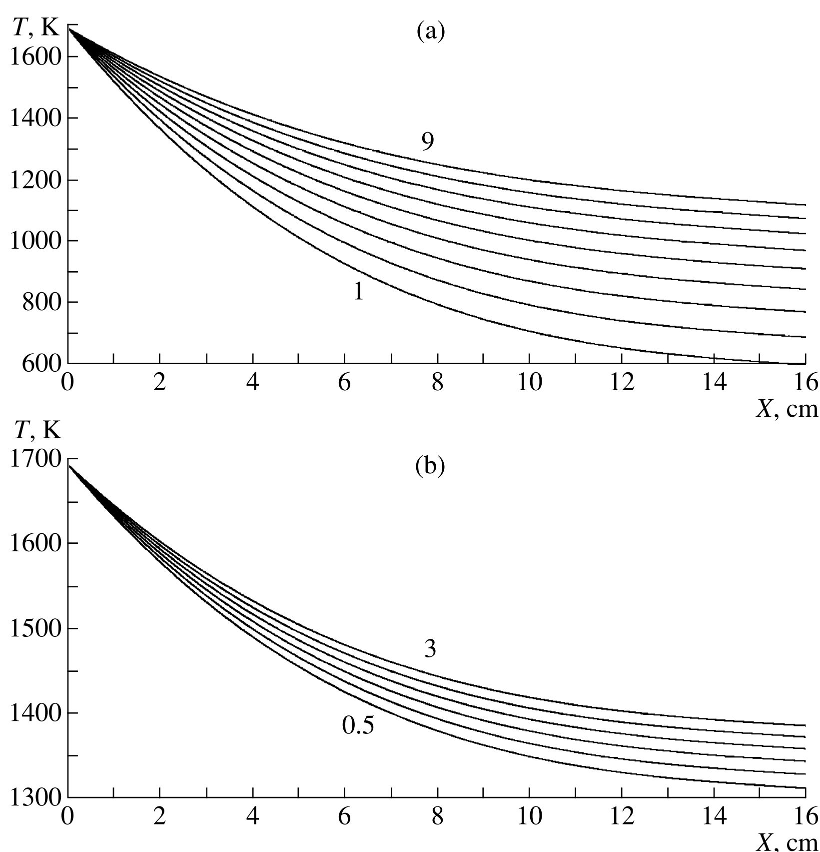

Fig. 1. Sets of $T(x)$ curves for (a) FZ-Si crystals grown at V = 1–9.0 mm/min and (b) CZ-Si crystals grown at V = 0.5–3 mm/min.

For the FZ-Si crystals, the dependence $T(x)$ was determined according to the empirical dependence [11]

$$\frac{dT}{dl} = 10 + (l - 16)^2 \exp(-61.2V - 0.28), \qquad (22)$$

where l is the distance (cm) from the crystallization front to the cross section under consideration and V is the crystal growth rate (cm/s).

To simplify the calculations, it was assumed for CZ-Si crystals that $G_{\text{FZ-Si}} \approx 3G_{\text{CZ-Si}}$, where G is the axial temperature gradient. At the same time, the expression for the temperature field can be set according to the results of [4]: $1/T = 1/T_m + Gx/T_m^2$, where T_m is the crystallization temperature and x is the distance from the crystallization front. For the FZ-Si and CZ-Si crystals, the dependences are given for V = 1–9 and 0.5–3 mm/min, respectively. In the first stage of the calculations, the radial temperature gradient was not taken into account and the radial defect distribution in the crystal was considered to be homogeneous.

The theoretical calculations were performed for the vacancy (O + V) and interstitial (C + I) branches of the heterogeneous mechanism of grown-in microdefect formation in FZ-Si and CZ-Si single crystals. Figures 2a and 2b show the calculated dependences of the concentrations of vacancies ($C_V/C_V(0)$) and oxygen–vacancy complexes ($C_{Q1}/C_{Q1}(0)$) on the CZ-Si crystal length in the range of growth rates from 0.5 to 3.0 mm/min (where $C_V(0)$ and $C_{Q1}(0)$ are, respectively, the concentrations of vacancies and complexes O + V near the crystallization front).

Similarly, Figs. 3a and 3b show the calculated dependences of the concentrations of interstitials ($C_I/C_I(0)$) and carbon–interstitial complexes ($C_{Q2}/C_{Q2}(0)$) on the FZ-Si crystal length in the range of growth rates from 1 to 9.0 mm/min (where $C_I(0)$ and $C_{Q2}(0)$ are, respectively, the concentrations of Si interstitials and (C + I) complexes near the crystallization front). The subscripts 1 and 2 indicate, respectively, the vacancy and interstitial branches of the heterogeneous mechanism of grown-in microdefect formation.

In the second stage of the calculations, a 2D temperature field was set in the analytical form according to the technique described in [12]: $1/T = 1/T_m + Gx/T_m^2$. The temperature field along the crystal surface is set as follows: $1/T = 1/T_m + G_a x/T_m^2$, where G_a is the axial temperature gradient along the crystal surface. Accord-

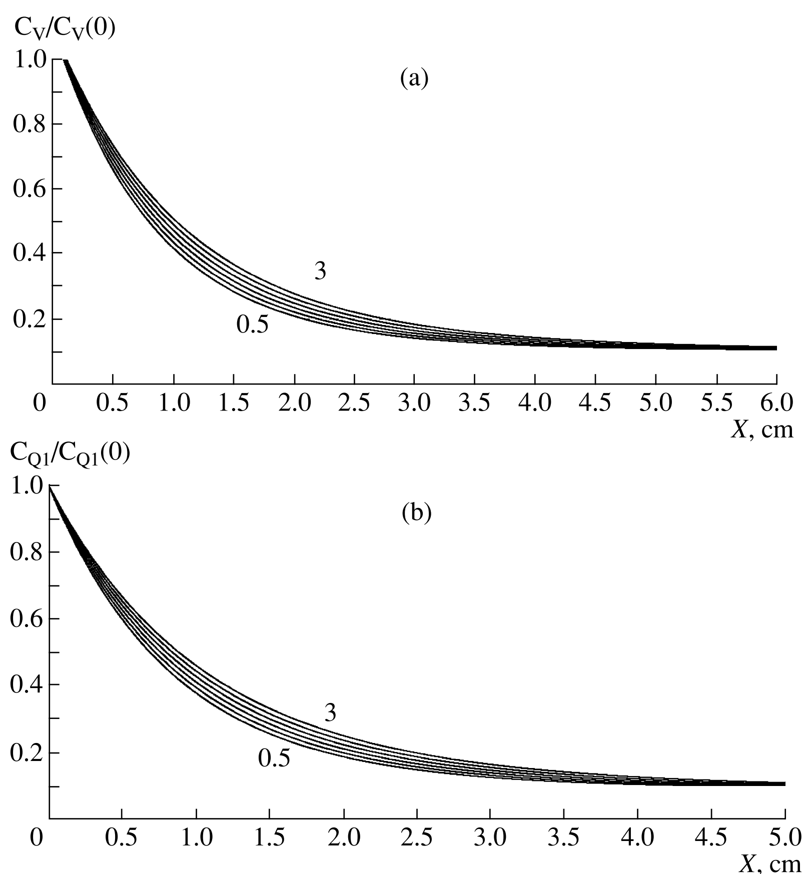

Fig. 2. Sets of the dependences of (a) $C_V/C_V(0)$ and (b) $C_{Q1}/C_{Q1}(0)$ on the crystal length for the CZ-Si crystals grown at V = 0.5–3 mm/min.

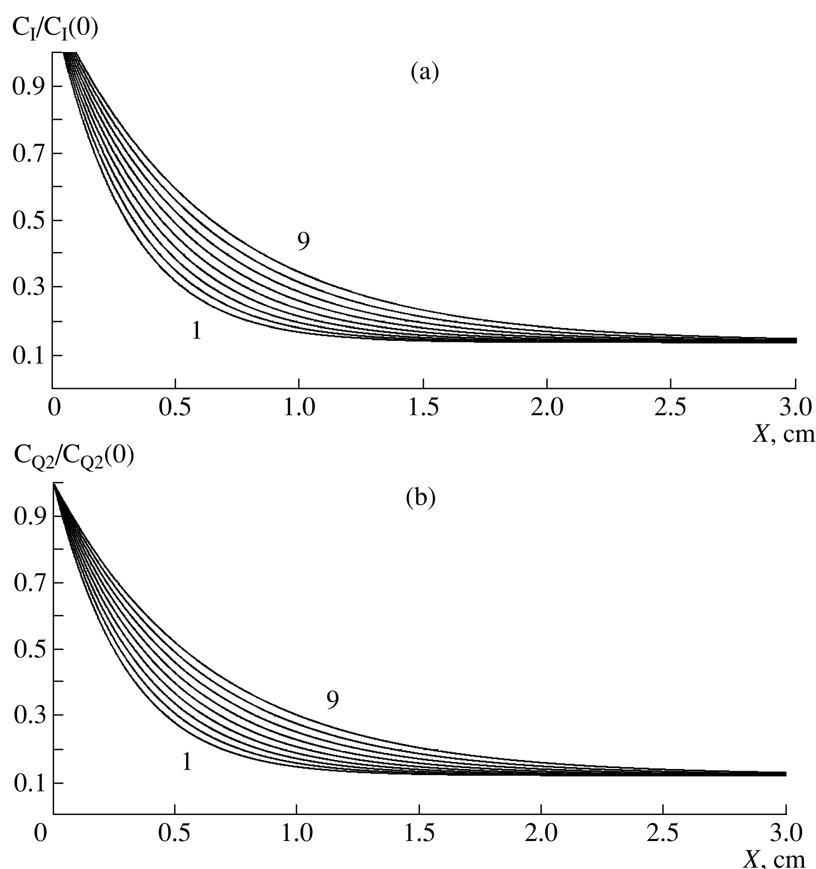

Fig. 3. Sets of the dependences of (a) $C_I/C_I(0)$ and (b) $C_{Q2}/C_{Q2}(0)$ on the crystal length for the CZ-Si crystals grown at V = 1–9.0 mm/min.

ing to the technique [12], the temperature field is set along the crystal axis and along its surface; the ratio of the field component along the surface to the component along the axis is varied with a certain step. At the crystallization front, G is varied for six growth rates of CZ-Si crystals (0.5–3 mm/min) and nine growth rates for FZ-Si crystals (1–9 mm/min). Eleven versions are considered in which the ratio $f = G_a/G = 1–2$ changes with a step of 0.1 according to [12].

The calculation data (see below) indicate that the results obtained by setting a 2D temperature field according to the technique [12], which was developed for large CZ-Si crystals, are similar to those obtained by us by setting the temperature field according to the technique [11], developed for compact FZ-Si crystals. The similarity of the results given by these two techniques indicates the absence of fundamental differences between them, their interchangeability, and the possibility of their application to crystals of any diameter.

Figures 4a and 4b show the sets of temperature distributions $T(x)$ along the crystal length for the FZ-Si (30 mm in diameter, V = 1–9 mm/min) and CZ-Si (50 mm in diameter, V = 0.5–3 mm/min) crystals. Figures 5a and 5b show the calculated dependences of $C_{Q1}(0)$ and $C_{Q2}(0)$ for vacancy–interstitial complexes in FZ-Si and CZ-Si crystals, respectively. Figures 6a and 6b present the radial distributions of the concentrations $C_{Q1}(0)$ and $C_{Q2}(0)$ for the FZ-Si and CZ-Si crystals, respectively.

4. DISCUSSION

Analysis of the calculated curves shows their good agreement with the experimental data and the results given by the heterogeneous mechanism of grown-in microdefect formation. This concerns the temperatures of formation of primary grown-in microdefects; experiments on crystal quenching (Table 1); and the concentrations of $(I + V)$ and D(C) microdefects (~10^{13}–10^{14} cm^{-3}), determined by electron microscopy [6, 7]. Therefore, despite the accepted assumptions, we can state that the dissociative model of impurity diffusion is in good agreement with the experimental data on grown-in microdefects and can serve as a theoretical basis of the heterogeneous mechanism of grown-in microdefect formation. The generation of secondary grown-in microdefects (interstitial dislocation loops, vacancy micropores) upon cooling of crystals below 1200°C can be caused by both the transformation of the initial struc-

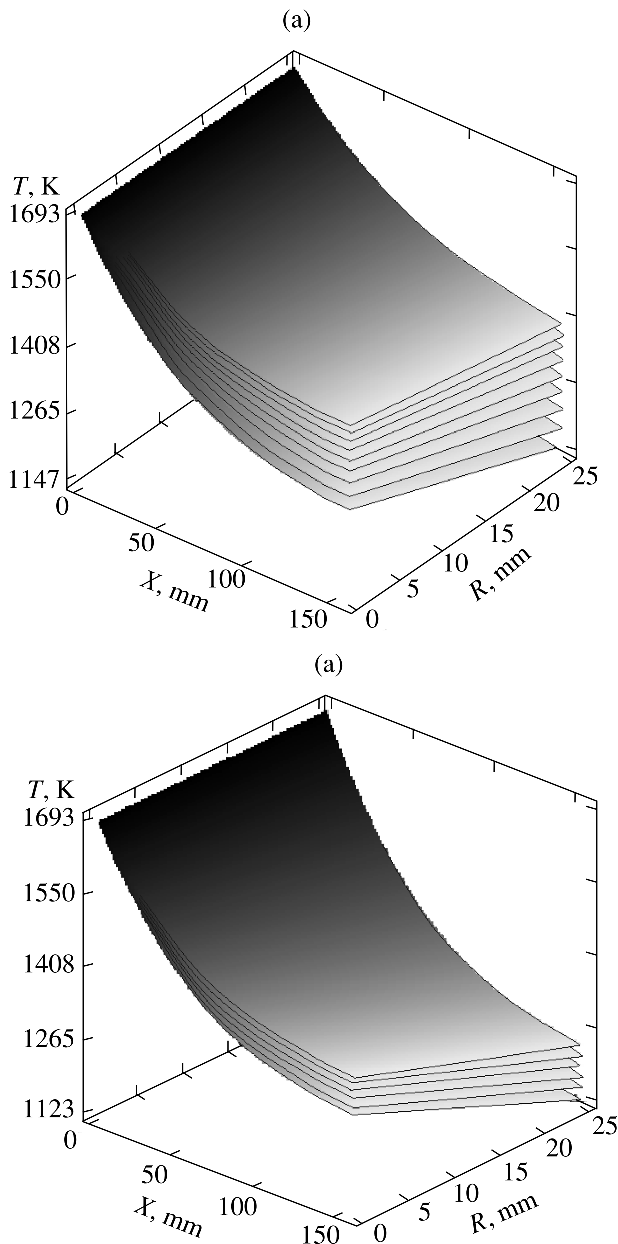

Fig. 4. Sets of the $T(x)$ planes for (a) FZ-Si crystals grown at V = 1–9.0 mm/min and (b) CZ-Si crystals grown at V = 0.5–3 mm/min.

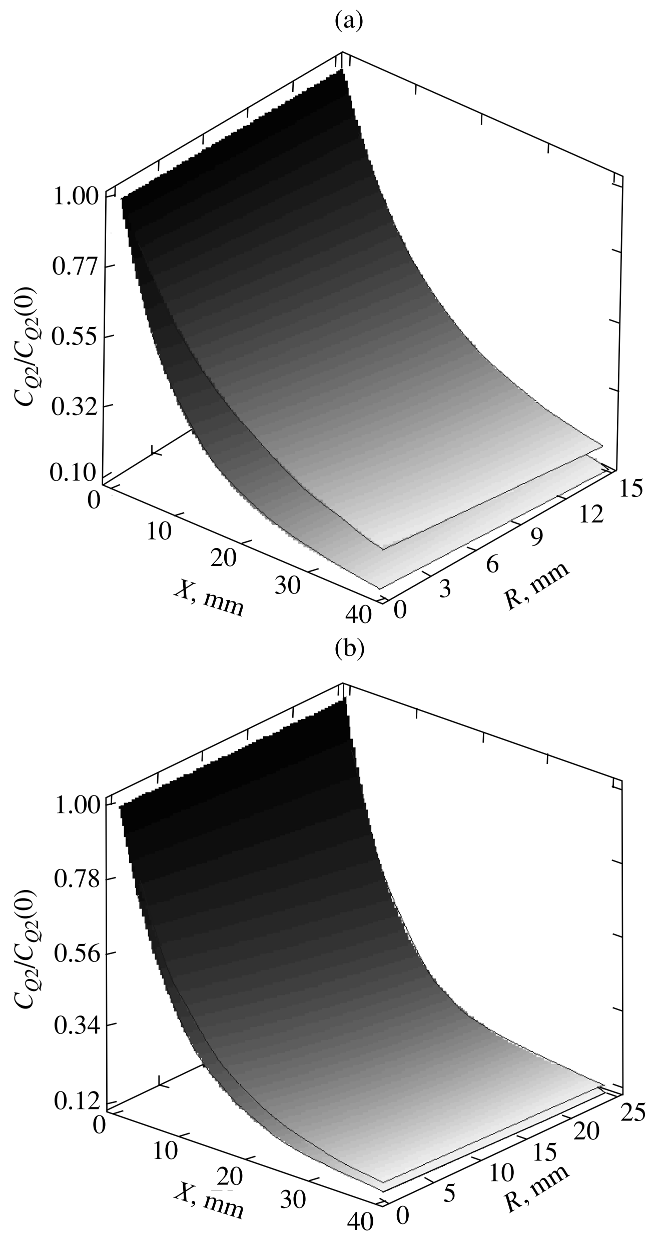

Fig. 5. Sets of the (a) $C_{Q1}/C_{Q1}(0)$ planes for the FZ-Si crystals and (b) $C_{Q2}/C_{Q2}(0)$ planes for the CZ-Si crystals.

ture of primary grown-in microdefects [6] and the formation of clusters of intrinsic point defects [7].

Note that vacancy pores were not experimentally found in compact dislocation-free Si single crystals (FZ-Si crystals 30 mm in diameter and CZ-Si crystals 50 mm in diameter) [6]. In our opinion, their absence is related to high cooling rates of these crystals at high growth rates. It is known that high cooling rates (≥40 K/min) suppress the formation of vacancy clusters and increase the density of oxygen precipitates [13].

Therefore, the process of interaction of intrinsic point defects with impurities, which begins near the crystallization front, has a fundamental (primary) character. It is decisive in the formation of the defect structure of dislocation-free Si single crystals of high structural quality. Upon cooling of a crystal (at $T < 1200°C$), depending on the thermal growth conditions, conditions for exceeding the equilibrium concentrations of intrinsic point defects arise owing to the impurity loss. As a result, vacancy micropores and interstitial dislocation loops are formed in different regions of the crystal.

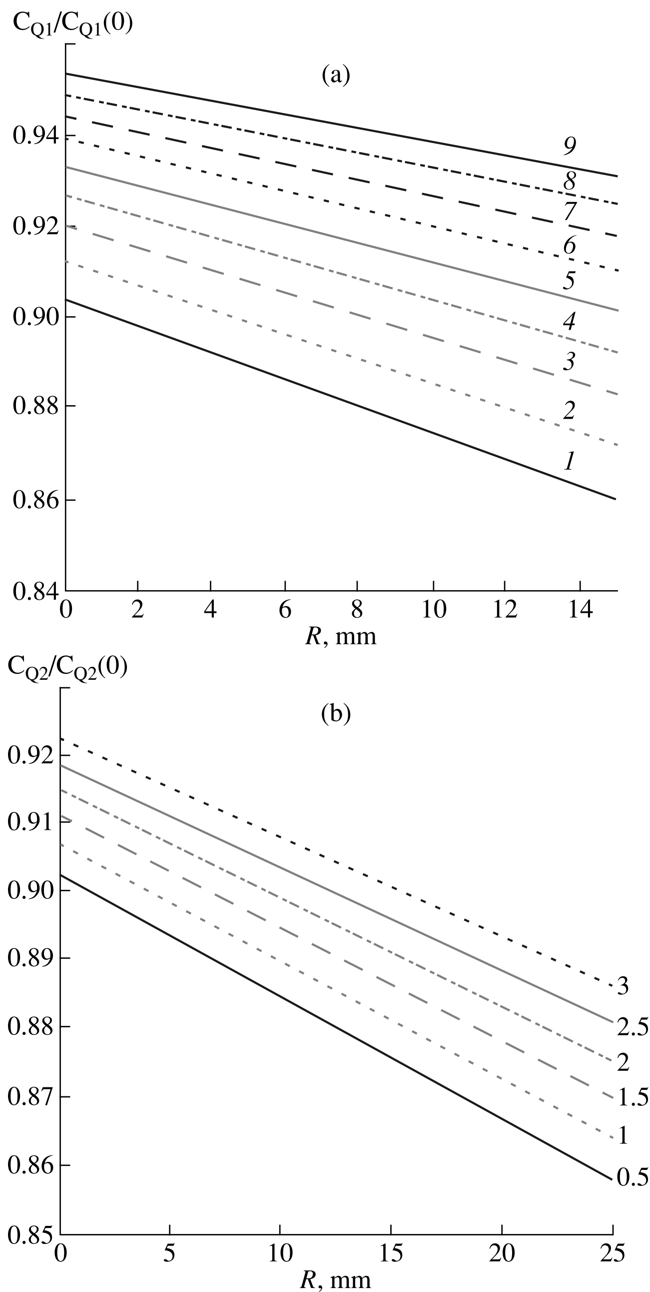

Fig. 6. Radial dependences of (a) $C_{Q1}/C_{Q1}(0)$ for the FZ-Si crystals and (b) $C_{Q2}/C_{Q2}(0)$ for the CZ-Si crystals; R is the crystal radius.

In this case, impurity precipitates can serve as condensation regions for intrinsic point defects.

CONCLUSIONS

A mathematical model of the formation of primary grown-in microdefects has been formulated on the basis of dissociative diffusion. The cases of oxygen–vacancy (O + V) and carbon–Si interstitial (C + I) interaction near the crystallization front are considered for dislocation-free Si single crystals grown by the floating-zone and Czochralski methods. The derived approximate analytical expressions are in agreement with the heterogeneous mechanism of grown-in microdefect formation.

The advantages of the proposed model for calculating the processes of defect formation during growth of dislocation-free Si single crystals are that it adequately describes the experimental data on grown-in microdefects and, in addition, is simple and available. The experimental and theoretical investigations showed that the defect formation is due to the point defect diffusion in the temperature gradient field. At temperatures close to the crystallization point, decomposition of supersaturated impurity solid solutions (primary grown-in microdefects) occurs. Upon crystal cooling (at $T < 1200°C$), supersaturated solid solutions of intrinsic point defects (secondary grown-in microdefects) decompose.

REFERENCES

1. M. S. Kulkarni, V. Voronkov, and R. Falster, J. Electrochem. Soc. **151**, 663 (2004).
2. T. Sinno and R. A. Brown, J. Electrochem. Soc. **146**, 2300 (1999).
3. E. Dornberger, von W. Ammon, J. Virbulis, et al., J. Cryst. Growth **230**, 291 (2001).
4. V. V. Voronkov, J. Cryst. Growth **59**, 625 (1982).
5. V. V. Voronkov and R. Falster, J. Electrochem. Soc. **149**, G167 (2002).
6. V. I. Talanin and I. E. Talanin, *New Research on Semiconductors*, Ed. by T. B. Elliot (Nova Sci. Publ, New York, 2006), p. 35.
7. V. I. Talanin and I. E. Talanin, Defect Diffusion Forum **230–232**, 177 (2004).
8. V. I. Talanin and I. E. Talanin, Izv. Vyssh. Uchebn. Zaved., Mater. Elektron. Tekh., No. 1, 14 (2006).
9. S. V. Bulyarskiĭ and V. I. Fistul', *Thermodynamics and Kinetics of Interacting Defects in Semiconductors* (Nauka, Moscow, 1997) [in Russian].
10. V. V. Vas'kin and V. A. Uskov, Fiz. Tverd. Tela (Leningrad) **10**, 1239 (1968) [Sov. Phys. Solid State **10**, 985 (1968)].
11. K. N. Neĭmark, B. A. Sakharov, V. F. Chulitskiĭ, and M. I. Osovskiĭ, *Silicon and Germanium* (Metallurgiya, Moscow, 1970), Issue 2 [in Russian].
12. N. A. Verezub, M. G. Mil'vidskiĭ, and A. I. Prostomolotov, Izv. Vyssh. Uchebn. Zaved., Mater. Elektron. Tekh., No. 2, 29 (2004).
13. K. Nakamura, I. Saishoji, and J. Tomioka, J. Cryst. Growth. **237–239**, 1678 (2002).

Translated by Yu. Sin'kov

SPELL: ok